The Astrophysical Journal, 690:1639–1647, 2009 January 10 doi:10.1088/0004-637X/690/2/1639


# MMT HYPERVELOCITY STAR SURVEY

Warren R. Brown, Margaret J. Geller, and Scott J. Kenyon
Smithsonian Astrophysical Observatory, 60 Garden St, Cambridge, MA 02138, USA; wbrown@cfa.harvard.edu, mgeller@cfa.harvard.edu, skenyon@cfa.harvard.edu
*Received 2008 July 30; accepted 2008 September 15; published 2008 December 22*

## ABSTRACT

We describe a new survey for unbound hypervelocity stars (HVSs), stars traveling with such extreme velocities that dynamical ejection from a massive black hole is their most likely origin. We investigate the possible contribution of unbound runaway stars, and show that the physical properties of binaries constrain low-mass runaways to bound velocities. We measure radial velocities for HVS candidates with the colors of early A-type and late B-type stars. We report the discovery of six unbound HVSs with velocities and distances exceeding the conservative escape velocity estimate of Kenyon and collaborators. We additionally report four possibly unbound HVSs with velocities and distances exceeding the lower escape velocity estimate of Xue and collaborators. These discoveries increase the number of unbound HVSs by 60%–100%. Other survey objects include 19 newly identified $z \sim 2.4$ quasars. One of the HVSs may be a horizontal branch star, consistent with the number of evolved HVSs predicted by Galactic center ejection models. Finding more evolved HVSs will one day allow a probe of the low-mass regime of HVSs and will constrain the mass function of stars in the Galactic center.

*Key words:* Galaxy: center – Galaxy: halo – Galaxy: kinematics and dynamics – Galaxy: stellar content – stars: early-type

*Online-only material:* color figures

## 1. INTRODUCTION

Three-body interactions with a massive black hole (MBH) will inevitably unbind stars from the Galaxy (Hills 1988; Yu & Tremaine 2003). In 2005 we reported the discovery of the first hypervelocity star (HVS): a 3 $M_\odot$ main-sequence star traveling with a Galactic rest-frame velocity of at least $+700 \pm 12$ km s$^{-1}$, more than twice the Milky Way's escape velocity at the star's distance of 110 kpc (Brown et al. 2005). This star cannot be explained by normal stellar interactions: the maximum ejection velocity from binary disruption mechanisms (Blaauw 1961; Poveda et al. 1967) is limited to $\lesssim 300$ km s$^{-1}$ for 3 $M_\odot$ stars (Leonard 1991, 1993; Tauris & Takens 1998; Portegies Zwart 2000; Davies et al. 2002; Gualandris et al. 2005). Although runaways may reach unbound velocities for very massive stars, like the hyper-runaway HD 271791 (Heber et al. 2008a; Przybilla et al. 2008a), runaway ejection velocities are constrained by the properties of binary stars. A massive and compact object is needed to accelerate low-mass stars to unbound velocities.

There is overwhelming evidence for a $\sim 4 \times 10^6$ $M_\odot$ MBH in the dense stellar environment of the Galactic center (Schödel et al. 2003; Ghez et al. 2008). Hills (1988) coined the term HVS to describe a star ejected by the MBH. The observational signature of an HVS is its unbound velocity. Although not all unbound stars are necessarily HVSs—fast-moving pulsars, for example, are explained by supernova kicks (e.g., Arzoumanian et al. 2002)—unbound low-mass main-sequence stars are most plausibly explained as HVSs.

Here we introduce a new HVS survey using the MMT to target HVS candidates with masses down to $\sim 2$ $M_\odot$. Discovering lower mass HVSs should provide constraints on the stellar mass function of HVSs (Brown et al. 2006a; Kollmeier & Gould 2007); the velocity distribution of low- versus high-mass HVSs may discriminate between a single MBH or binary MBH origin (Sesana et al. 2007b; Kenyon et al. 2008). Our survey strategy targets stars that are fainter and redder than the original HVS survey. This strategy is successful: we report the discovery of six unbound HVSs and four possibly unbound HVSs.

### 1.1. Recent Observations of HVSs

Observers have identified a remarkable number of HVSs in the past three years. Following the discovery of the first HVS (Brown et al. 2005), Hirsch et al. (2005) reported a helium-rich subluminous O star leaving the Galaxy with a rest-frame velocity of at least +717 km s$^{-1}$. Edelmann et al. (2005) reported a 9 $M_\odot$ main-sequence B star with a Galactic rest-frame velocity of at least +548 km s$^{-1}$, possibly ejected from the Large Magellanic Cloud (LMC). Brown et al. (2006a, 2006b, 2007a, 2007b) reported seven B-type HVSs discovered in a targeted HVS survey, along with evidence for an equal number of bound HVSs ejected by the same mechanism.

High-dispersion spectroscopy has shed new light on the nature of the HVSs. Przybilla et al. (2008c) have recently shown that HVS7 is a chemically peculiar B main-sequence star, with an abundance pattern unusual even for the class of peculiar B stars. The star HVS3 (HE 0437-5439), the unbound HVS very near to the LMC on the sky, has received the most attention. HVS3 is a 9 $M_\odot$ B star of half-solar abundance, a good match to the abundance of the LMC (Bonanos et al. 2008; Przybilla et al. 2008b). Stellar abundance, however, may not be conclusive evidence of origin. A- and B-type stars exhibit 0.5–1 dex scatter in elemental abundances within a single cluster, due to gravitational settling and radiative levitation in the atmospheres of the stars (Varenne & Monier 1999; Monier 2005; Fossati et al. 2007; Gebran et al. 2008; Gebran & Monier 2008).

An LMC origin requires that HVS3 was ejected from the galaxy at $\sim 1000$ km s$^{-1}$ (Przybilla et al. 2008b), a velocity that can possibly come from three-body interactions with an intermediate-mass black hole in a massive star cluster (Gualandris & Portegies Zwart 2007; Gvaramadze et al. 2008). Perets (2008) shows that the ejection rate of 9 $M_\odot$ stars, however,

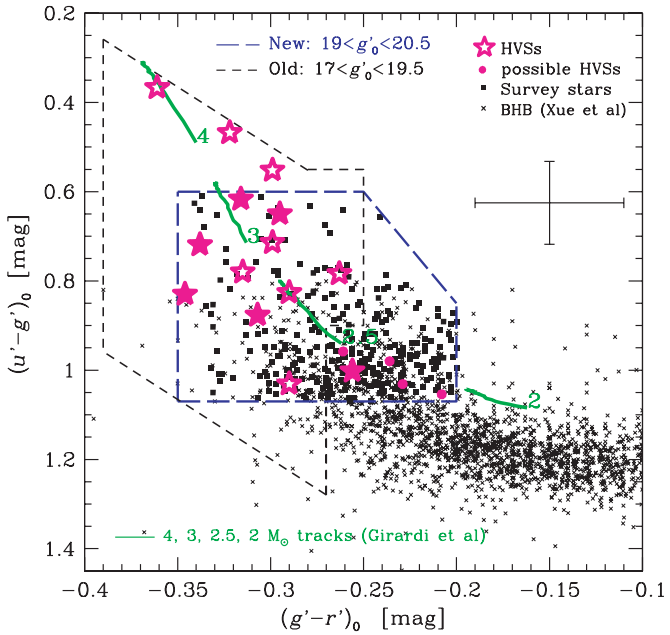


**Figure 1.** Color–color diagram illustrating the target selection for our new HVS survey (long dashed line) and our old HVS survey (short dashed line). The six new HVSs (solid stars) and four possible HVSs (solid dots) scatter around the Girardi et al. (2004) stellar evolution tracks for 2–4 $M_\odot$ main-sequence stars (solid lines). Average color uncertainties are indicated by the errorbar on the upper right. Previous HVS discoveries (open stars) and the Xue et al. (2008) BHB sample (x's) are also marked.

(A color version of this figure is available in the online journal.)

is four orders of magnitude too small for this explanation to be plausible. The alternative explanation is that HVS3 is a blue straggler, ejected by the Milky Way's MBH. Theorists argue that a single MBH or a binary MBH can eject a compact binary star as an HVS (Lu et al. 2007; Perets 2008); the subsequent evolution of such a compact binary can result in mass transfer and/or a merger that can possibly explain HVS3 (Perets 2008). Proper motion measurements, underway now, will determine HVS3's origin.

Other recent HVS work highlights the link between stellar rotation and the origin of HVSs. Main-sequence B stars have fast mean $v \sin i \sim 150$ km s$^{-1}$ (e.g., Abt et al. 2002; Huang & Gies 2006). Hot blue horizontal branch (BHB) stars have slow mean $v \sin i < 10$ km s$^{-1}$ because they have just evolved off the red giant branch (e.g., Behr 2003a, 2003b). Interestingly, Hansen (2007) predicts that main-sequence HVSs ejected by the Hills mechanism should be slow rotators, because stars in compact binaries have systematically lower $v \sin i$ due to tidal synchronization. Löckmann & Baumgardt (2008), on the other hand, predict that HVSs should be fast rotators, at least for single stars spun up and ejected by a binary black hole. To date HVS1, HVS3, HVS7, and HVS8 have observed $v \sin i$ of ∼190, $55 \pm 2$, $55 \pm 2$, and $260 \pm 70$ km s$^{-1}$, respectively (Heber et al. 2008b; Przybilla et al. 2008b, 2008c; Lopez-Morales & Bonanos 2008). As discussed by Perets (2009), we clearly require a larger sample of HVSs to measure the distribution of HVS rotations and discriminate HVS ejection models.

In Section 2 we describe our new HVS survey strategy and summarize our observations. In Section 3 we discuss the Galactic escape velocity, our definition of an HVS, and the possible contribution of hyper-runaways to the population of unbound stars. In Section 4 we present the new unbound HVSs. In Section 5 we discuss a possible BHB star among the HVSs. We conclude in Section 6.

## 2. DATA

### 2.1. New Target Selection

HVSs are rare: our discoveries imply that there are $96 \pm 20$ HVSs of mass 3–4 $M_\odot$ within 100 kpc (Brown et al. 2007b). Thus to find new HVSs we must target luminous objects over a very large volume. Luminous O- and B-type HVSs, even if they lived long enough to be observed, would be lost behind a large foreground of hot white dwarfs with identical colors, $(u'-g')_0 \lesssim 0.4$. We design our new HVS survey to target early A-type stars.

Known HVSs are located at distances 50–100 kpc, corresponding to $19.5 < g'_0 < 21$ for early A-type stars. At such magnitudes, fewer than ∼ 100 A-type stars have published radial velocities (Sirko et al. 2004a; Clewley et al. 2005; Xue et al. 2008). Halo BHB and blue straggler stars are a major contaminant at faint magnitudes, but fortunately the density of the stellar halo falls off very steeply. Kenyon et al. (2008) calculate that the density profile of unbound HVSs is approximately $\rho \propto r^{-2}$ (see also Kollmeier & Gould 2007); the density profile of the stellar halo is closer to $\rho \propto r^{-3}$ (e.g., Jurić et al. 2008). Thus we maximize the contrast of HVSs with respect to indigenous halo stars by restricting ourselves to the faintest A-stars.

We select candidate HVSs in the magnitude range $19.0 < g'_0 < 20.5$. The faint limit is set by the Sloan Digital Sky Survey (SDSS) photometric errors, which approach ±0.15 in $(u'-g')_0$ at $g' = 20.5$. The bright limit is set to provide continuity with our original HVS survey, although we impose a more stringent bright limit on the reddest stars $g'_0 > 18.6+10[(g'-r')_0+0.3]+[(u'-g')_0-(1.2(g'-r')_0+1.25)]$. In other words, $g'_0 > 19.5$ at $(g'-r')_0 = -0.2$. We use a combination of $(u'-g')_0$ and $(g'-r')_0$ colors to select stars with probable high surface gravity, and thus maximize the chance of finding main-sequence HVSs.

Figure 1 illustrates the color selection. The original HVS survey (dashed line) was designed to avoid the locus of BHB/A-type stars; our new HVS survey (long dashed line) follows the Girardi et al. (2002, 2004) main-sequence tracks for solar abundance stars (solid lines) down to ∼ 2 $M_\odot$ A-stars. Known HVSs scatter uniformly around the main-sequence tracks. Known BHB stars (Xue et al. 2008), on the other hand, are systematically redder in $(u'-g')_0$.

We select stars with $0.6 < (u'-g')_0 < 1.07$ to avoid the majority of known halo BHB stars (Figure 1). We select stars with $-0.35 < (g'-r')_0 < -0.20$ to include 3 $M_\odot$ stars that can viably travel 150 kpc (= 20.5 mag) in their main-sequence lifetimes. Finally, we impose $-0.5 < (r'-i')_0 < 0$ and $(g'-r')_0 < 0.2(u'-g')_0 - 0.38$ to exclude nonstellar objects, such as quasars. Notably, this color selection includes the first HVS, which was not formally a part of the original HVS survey.

Applying this color–magnitude selection to the SDSS DR6 photometric catalog results in 528 HVS candidates spread over 7300 deg$^2$. We have excluded the small region of the SDSS between $b < -l/5 + 50°$ and $b > l/5 - 50°$ to avoid excessive contamination from Galactic bulge stars. Of the 528 HVS candidates, 59 were previously observed as part of our original HVS survey (Brown et al. 2007b), and 21 are in the Sirko et al. (2004a) BHB catalog. Thus we need spectra for 448 HVS candidates.

### 2.2. Spectroscopic Observations

Spectroscopic observations were obtained at the 6.5m MMT telescope with the Blue Channel spectrograph on the nights

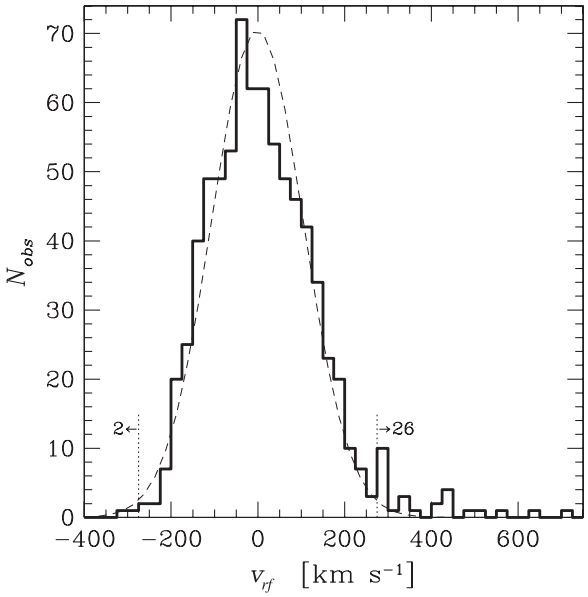


**Figure 2.** Minimum Galactic rest-frame velocity $v_{rf}$ distribution for the 759 stars in the combined HVS survey. The best-fit Gaussian (dashed line) has dispersion of $106 \pm 5$ km s$^{-1}$, excluding the 26 stars with $v_{rf} > +275$ km s$^{-1}$. The asymmetry of positive velocity outliers is significant at the $\sim 4\sigma$ level and shows that the +300 km s$^{-1}$ stars are short lived; we observe only two stars falling back onto the Galaxy around $-300$ km s$^{-1}$.

of 2008 February 6–10 and 2008 May 7–11. We operated the spectrograph with the 832 line mm$^{-1}$ grating in second order and a 1.″25 slit. These settings provide wavelength coverage of 3650–4500 Å and a spectral resolution of 1.2 Å. All observations were obtained at the parallactic angle.

Our goal was to obtain modest signal-to-noise ratio (S/N) observations adequate for determining radial velocity. We typically obtained S/N = 5 in the continuum at 4000 Å in a 10 minute integration on a $g' = 20$ star. We obtained spectra for 233 HVS candidates, and processed the data in real time to allow additional observations of interesting candidates. We extracted the spectra using IRAF[1] in the standard way and measured radial velocities using the cross-correlation package RVSAO (Kurtz & Mink 1998). The average radial velocity uncertainty of the S/N = 5 spectra is $\pm 20$ km s$^{-1}$.

### 2.3. HVS Sample

We now have spectroscopic identifications and radial velocities for 313 (59%) of the 528 HVS candidates. Nineteen of the objects are newly identified $z \sim 2.4$ quasars, and nine of the objects are DA white dwarfs. We present the quasars and white dwarfs in Appendix. The remaining 285 objects have the spectra of early A- and late B-type stars. In addition, we observed the final 40 objects remaining in the original HVS survey (Brown et al. 2007b).

Because our new and original HVS surveys cover contiguous regions of color–magnitude space over the same region of sky, we consider the results of the combined surveys in this paper. We exclude stars with $g'_0 < 17$ that are possibly associated with the inner halo; the inner halo has distinctly different kinematics from the outer halo (Carollo et al. 2007; Morrison et al. 2008). We also exclude all white dwarfs, quasars, and B supergiants. Our combined HVS survey contains 759 nonkinematically-selected stars $17 < g'_0 < 20.5$.

### 2.4. Radial Velocity Distribution

Figure 2 plots the distribution of line-of-sight velocities, corrected to the Galactic rest frame (see Brown et al. 2006b), for the combined sample of 759 stars. The 731 survey stars with $|v_{rf}| < 275$ km s$^{-1}$ have a $-1 \pm 4$ km s$^{-1}$ mean and a $106 \pm 5$ km s$^{-1}$ dispersion, consistent with a normal stellar halo population. Notably, there are 28 stars in the tails of the distribution with $|v_{rf}| > 275$ km s$^{-1}$.

We observe 26 stars with $v_{rf} > 275$ km s$^{-1}$ and only two stars with $v_{rf} < -275$ km s$^{-1}$. The escape velocity of the Milky Way at 50 kpc is $\sim 360$ km s$^{-1}$ (Kenyon et al. 2008), thus the 12 stars with $v_{rf} > 400$ km s$^{-1}$ are unbound. Ignoring the 12 unbound stars, there is less than a $10^{-5}$ probability of randomly drawing 14 stars with 275 km s$^{-1}$ $< v_{rf} < 400$ km s$^{-1}$ from the tail of a Gaussian distribution with the observed parameters. Thus the excess of positive velocity outliers 275 km s$^{-1}$ $< v_{rf} < 400$ km s$^{-1}$ appear significant at the $4\sigma$ level.

The positive velocity outliers demonstrate a population of short-lived HVSs ejected onto bound trajectories (Brown et al. 2007a, 2007b). HVS ejection mechanisms naturally produce a broad spectrum of ejection velocities (e.g., Sesana et al. 2007b). Simulations of HVS ejections from the Hills mechanism suggest that there should be comparable numbers of unbound and bound HVSs with $v_{rf} > +275$ km s$^{-1}$ in our survey volume (Bromley et al. 2006). As shown below, we find 14 unbound HVSs and 12 possibly bound HVSs with $v_{rf} > +275$ km s$^{-1}$, in good agreement with model predictions.

## 3. UNBOUND STARS

### 3.1. Defining Hypervelocity Stars

Following Hills (1988), we define HVSs by (1) their MBH origin and (2) their unbound velocities. An HVS ejected from the Milky Way travels on a nearly radial trajectory; the expected proper motion for a 50 kpc distant HVS is a few tenths of a milliarcsecond per year (e.g., Gnedin et al. 2005). Thus radial velocity directly measures most of a HVS's space motion. Deciding whether a HVS is unbound, however, requires knowledge of the star's distance.

We estimate distances to the HVSs assuming that they are main-sequence stars. This assumption is motivated by the significant absence of stars falling back onto the Galaxy around $-300$ km s$^{-1}$ (Figure 2). Bound HVSs must have main-sequence lifetimes less than $\sim$1 Gyr, otherwise we would see them falling back onto the Galaxy (Brown et al. 2007b; Kollmeier & Gould 2007; Yu & Madau 2007). Given the color selection of our survey (Figure 1), the A- and B-type HVSs must be 2–4 $M_\odot$ main-sequence stars at Galactocentric distances $> 40$ kpc.

Unfortunately, the Galactic potential is poorly constrained at distances $> 40$ kpc. We consider two Galactic potential models here. Kenyon et al. (2008) discuss a spherically symmetric potential that, for the first time, fits the Milky Way mass distribution from 5 pc to $10^5$ pc. Because the form of the potential does not yield a true escape velocity, Kenyon et al. (2008) define unbound stars as having $v_{rf} > 200$ km s$^{-1}$ at $R = 150$ kpc. This conservative definition yields a Galactic escape velocity of 360 km s$^{-1}$ at 50 kpc and 260 km s$^{-1}$ at 100 kpc (Figure 3). Xue et al. (2008), on the other hand, fit a halo

[1] IRAF is distributed by the National Optical Astronomy Observatories, which are operated by the Association of Universities for Research in Astronomy, Inc., under cooperative agreement with the National Science Foundation.

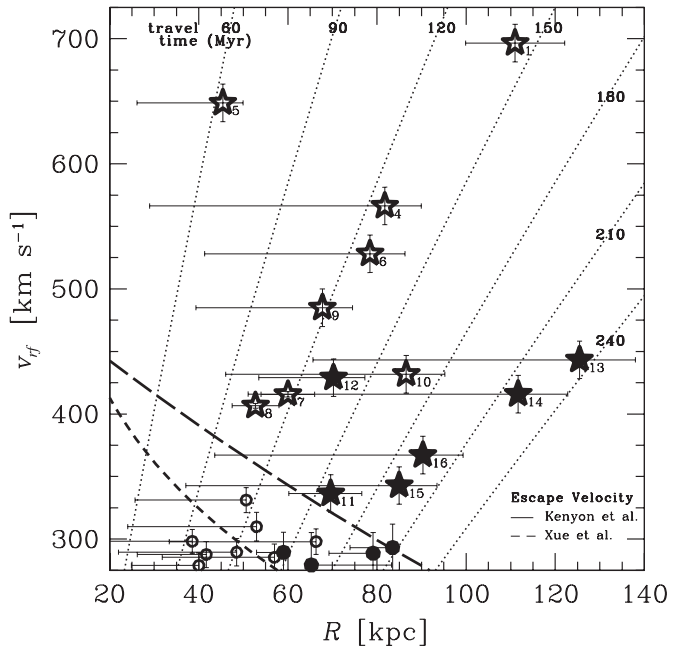


**Figure 3.** Minimum rest-frame velocity vs. Galactocentric distance $R$ for the 26 stars with $v_{rf} > +275$ km s$^{-1}$. The six new HVSs (solid stars) have velocities and main-sequence star distances exceeding the Kenyon et al. (2008) escape velocity model (long dashed line). Four possible HVSs (solid dots) have velocities, main-sequence star distances, and BHB distances exceeding the Xue et al. (2008) escape velocity model (dashed line). Previous HVS discoveries (open stars) and possibly bound HVSs (open circles) are also indicated. Errorbars show the span of physically plausible distance if the HVSs were BHB stars. Isochrones of travel time from the Galactic center (dotted lines) are calculated using the potential model of Kenyon et al. (2008), assuming the observed minimum rest-frame velocity $v_{rf}$ is the full space motion of the stars.

potential model to the velocity dispersion of 2466 BHB stars located 5 kpc $< R <$ 60 kpc. The escape velocity resulting from the Xue et al. (2008) model is 290 km s$^{-1}$ at 50 kpc and 190 km s$^{-1}$ at 100 kpc (Figure 3).

### 3.2. Hyper-Runaways

Not all unbound stars are HVSs. The star HD 271791 is the first example of an unbound hyper-runaway that was ejected from the outer disk, in the direction of Galactic rotation, when its former 55 $M_\odot$ binary companion exploded as a supernova (Heber et al. 2008a; Przybilla et al. 2008a). Objects ejected in this manner are traditionally called runaways (Blaauw 1961). The term runaway also includes stars dynamically ejected from binary–binary encounters (Poveda et al. 1967).

We investigate here the possible contribution of runaways to the population of HVSs. First, we consider the properties of binaries required to produce unbound hyper-runaways. Then, we consider the production rate of stars massive enough to produce these hyper-runaways.

#### 3.2.1. Binary Star Properties

Both the supernova and binary–binary ejection mechanisms share a common velocity constraint: the physical properties of binary stars. Theoretically, the maximum ejection velocity from disrupting a binary (e.g., by a supernova) is the binary orbital velocity. The maximum ejection velocity from dynamical binary–binary encounters is the escape velocity of the most massive star, which for stars on the upper main sequence is $v_{\rm esc} \simeq 700(M/M_\odot)^{0.15}$ km s$^{-1}$ (Leonard 1991). This theoretical maximum ejection velocity is not realizable, however, because compact binaries that are too tight will merge instead of producing a runaway (Fregeau et al. 2004).

To avoid merging, a compact binary must avoid losing too much energy from Roche lobe overflow and from tidal dissipation. Stars with separations less than 2.5 $R_{\rm star}$ overfill their Roche lobes and quickly merge (e.g., Vanbeveren et al. 1998). During close binary encounters, tidal dissipation can lead to mergers of compact binaries (Lee & Ostriker 1986; McMillan et al. 1987; Leonard & Duncan 1988). These mechanisms are especially problematic for binaries involving a supernova. When a massive primary star evolves (prior to exploding), it experiences significant mass loss. Dynamical friction from the primary's wind causes the secondary star to quickly inspiral, thus conserving the angular momentum of the system (Vanbeveren et al. 1998). A minimum binary separation must be chosen to prevent mergers. Unfortunately, the details of tidal dissipation and stellar merging are uncertain. Thus we make only optimistic assumptions in our estimate of hyper-runaway ejection rates.

#### 3.2.2. Hyper-Runaway Ejection Rate

In the context of our HVSs, a runaway must have a velocity exceeding 400 km s$^{-1}$ to be confused with an HVS. The orbital velocity of the secondary star in a binary is

$$v_{\rm sec} = \frac{2\pi a}{(1+q)P}, \quad (1)$$

where $a$ is the separation of the two stars, $q = M_2/M_1$ is the mass ratio, and $P$ is the orbital period. We insert Kepler's third law $P^2 = 4\pi^2 a^3/(GM)$ into Equation 1, set $v_{\rm sec} \geqslant 400$ km s$^{-1}$, and find that the progenitor binary system must have

$$M/a \geqslant 0.84(1+q)^2(M_\odot/R_\odot) \quad (2)$$

to produce $a \geqslant 400$ km s$^{-1}$ runaway. Here, $M$ is the total mass of the binary. We will optimistically assume that the secondary fills its Roche lobe and has a radius of $\sim 0.4a$. Because a 3 $M_\odot$ star has a 3 $R_\odot$ radius, a binary must have $a \geqslant 8$ $R_\odot$ and a primary star with mass $\geqslant$10 $M_\odot$ to produce the requisite 3 $M_\odot$ runaway ejected at $\geqslant 400$ km s$^{-1}$ (Equation 2).

Known HVSs have travel times spanning 200 Myr (see Figure 3). The star formation rate in the solar neighborhood is 0.5 $M_\odot$ yr$^{-1}$ (Lada & Lada 2003). Thus $10^8$ $M_\odot$ of stars have formed in the disk in the past 200 Myr.

A standard Salpeter initial mass function (Salpeter 1955), integrated from 0.1 $M_\odot$ to 100 $M_\odot$ and normalized to $10^8$ $M_\odot$, predicts $5.4 \times 10^5$ stars with masses 10–100 $M_\odot$. All O and B stars are in binaries, and a third of the binaries are twins (Kobulnicky & Fryer 2007). Thus $1.8 \times 10^5$ of massive primaries are not twins. Assuming the secondaries have a Salpeter mass function (Kobulnicky & Fryer 2007), there are $\sim$600 secondaries with mass 3–4 $M_\odot$. Given a log-normal distribution of binary separations, $\sim$5% of binaries have 8–20 $R_\odot$ semimajor axes enabling a $\geqslant 400$ km s$^{-1}$ ejection. Thus we expect $\sim$30 3–4 $M_\odot$ runaways ejected at $\geqslant 400$ km s$^{-1}$ in the past 200 Myr.

The Galactic disk has an exponential stellar density profile with radial scale length 2.4 kpc (Siegel et al. 2002). Thus the region of the outer disk 10 kpc $< R <$ 20 kpc, despite containing most of the disk's area, contains no more than 10% of the disk's stars if we optimistically normalize the density over 5 kpc $< R <$ 20 kpc. Thus we predict only $\sim$3 possible 3–4 $M_\odot$ hyper-runaways ejected from the outer disk in the past 200 Myr.

However, potential models of the Milky Way show that a star traveling with 400 km s$^{-1}$ in the region 10 kpc $< R <$ 20 kpc is bound (see Figure 3). To achieve an unbound velocity, a runaway must be ejected at 400 km s$^{-1}$ in the direction of Galactic rotation. Assuming that runaways are ejected in random directions, no more than 10% of ejections will be in the direction of Galactic rotation. Thus we predict ∼0.3 hyper-runaways with mass 3–4 $M_\odot$ were ejected in the past 200 Myr, preferentially found at low Galactic latitudes.

The ejection rate from binary–binary encounters is even smaller, because it depends on the joint probability of colliding two compact binaries. A cluster of $10^5$ stars following a Salpeter mass function contains 330 3–4 $M_\odot$ stars and 190 10–100 $M_\odot$ stars. We optimistically assume that the 330 3–4 $M_\odot$ stars are in 330 different binaries, and that the 10–100 $M_\odot$ stars are in 130 binaries (because a third of them are twins; Kobulnicky & Fryer 2007). A log-normal distribution of binary separation suggests that ∼5% of the binaries have 8–20 $R_\odot$ semimajor axes enabling a $\geqslant$ 400 km s$^{-1}$ ejection. This reduces the number of relevant binaries containing 3–4 $M_\odot$ and 10–100 $M_\odot$ stars to 17 and seven, respectively. If mass segregation puts all of the compact binaries in the central 0.1 pc, then the space density of compact binaries containing a 10–100 $M_\odot$ star is $2 \times 10^3$ pc$^{-3}$. If we assume a velocity dispersion of 1 km s$^{-1}$ and a cross section for collision of $r = 20R_\odot$, then the ejection rate of 3–4 $M_\odot \geqslant 400$ km s$^{-1}$ runaways is $\sim 2 \times 10^{-8}$ Myr$^{-1}$ per cluster. Because 10 $M_\odot$ stars live ∼20 Myr (e.g., Schaller et al. 1992), and because we require ∼3000 clusters to reach $10^8$ $M_\odot$, we expect $\sim 10^{-3}$ binary–binary runaways with mass 3–4 $M_\odot$ and ejection velocity $\geqslant$ 400 km s$^{-1}$ in the past 200 Myr. However, these binary–binary runaways are subject to the same outer disk and Galactic rotation constraints as the supernova runaways. Thus we predict that only $\sim 10^{-5}$ 3–4 $M_\odot$ *hyper*-runaways were ejected by binary–binary encounters in the past 200 Myr.

In contrast, our HVS discoveries imply 96 ± 20 unbound 3–4 $M_\odot$ stars were ejected over the same time period. We conclude that 3–4 $M_\odot$ HVSs ejected from the Galactic Center are $\gtrsim$ 100 times more common than hyper-runaways of the same mass.

Hyper-runaways are rare because of the rarity of massive stars and compact binaries, and the requirement to avoid merging the compact binary progenitors. Hyper-runaways are also preferentially located at low Galactic latitudes. While it is possible for a hyper-runaway to be confused with an HVS in the absence of proper motions, the observed ∼3 $M_\odot$ unbound stars are almost certainly HVSs ejected by the central MBH.

## 4. NEW HYPERVELOCITY STARS

### *4.1. Six Unbound HVSs*

Here we describe the six unbound HVSs newly discovered in our survey. The first two stars are of later spectral type than the HVS discoveries in our previous targeted survey (Brown et al. 2006a, 2006b, 2007a, 2007b).

SDSS J095906.48+000853.40, hereafter HVS11, has an A1 spectral type, a +482 ± 19 km s$^{-1}$ heliocentric radial velocity, and a minimum velocity of +336 km s$^{-1}$ in the Galactic rest frame. An A-type spectral classification is supported by a strong λ3933 Ca II K line in the spectrum (Figure 4). HVS11 is the reddest HVS identified to date, with a broadband color $(g' - r')_0 = -0.256 \pm 0.028$. A solar metallicity 2.5 $M_\odot$ main-sequence star has $M_V(2.5\ M_\odot) \simeq +0.6$ (Schaller et al. 1992).

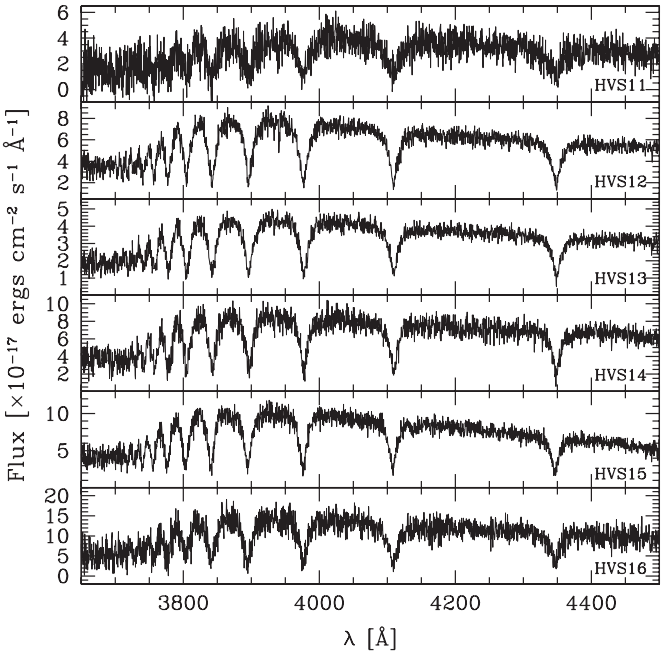


**Figure 4.** Observed MMT spectra of the six new HVSs.

This luminosity places HVS11 at an approximate Galactocentric distance $R = 70$ kpc.

Known HVSs are typically separated by 10°–20° from the nearest Local Group dwarf galaxy, however HVS11 is only 3.°9 from the Sextans dwarf. Any physical association with Sextans is very unlikely. Sextans is 1320 ± 40 kpc distant (Dolphin et al. 2003) and has a heliocentric velocity of 224 ± 2 km s$^{-1}$ (Young 2000). Thus HVS11 is moving towards the dwarf galaxy with a relative velocity of +260 km s$^{-1}$.

SDSS J105009.60+031550.67, hereafter HVS12, has an A0 spectral type, a +552 ± 11 km s$^{-1}$ heliocentric radial velocity, and a minimum velocity of +429 km s$^{-1}$ in the Galactic rest frame. HVS12 has a strong λ3933 Ca II K line and a higher S/N spectrum than HVS11 (Figure 4). We measure a 0.8 ± 0.1 equivalent width of Ca II K. Combining Ca II K with the star's broadband color $(g' - r')_0 = -0.307 \pm 0.039$, equivalent to $(B - V)_0 = -0.05$ (Clewley et al. 2005), we estimate [Fe/H]= −0.5 ± 0.7 (Wilhelm et al. 1999). HVS12 is therefore consistent with being a solar metallicity 2.5 $M_\odot$ main-sequence star, placing it at an approximate Galactocentric distance $R = 70$ kpc.

SDSS J105248.31−000133.94, hereafter HVS13, has a +575 ± 11 km s$^{-1}$ heliocentric radial velocity and a minimum velocity of +443 km s$^{-1}$ in the Galactic rest frame. Although its $(g' - r')_0 = -0.295 \pm 0.034$ is nearly identical to HVS12, HVS13 is 0.23 mag bluer in $(u' - g')_0$ and has a B9 spectral type (Figure 4) consistent with a 3 $M_\odot$ main-sequence star (see also Figure 1), the same spectral type observed for most of the other HVSs in our survey. At $g = 20.18 \pm 0.02$, however, HVS13 is the faintest HVS discovered to date. A solar metallicity 3 $M_\odot$ main-sequence star has $M_V \simeq -0.3$ (Schaller et al. 1992), which places HVS13 at $R = 125$ kpc.

SDSS J104401.75+061139.03, hereafter HVS14, has a B9 spectral type, a 532 ± 13 km s$^{-1}$ heliocentric radial velocity, and a minimum velocity of 416 km s$^{-1}$ in the Galactic rest frame. Its broadband colors are consistent with a 3 $M_\odot$ main-sequence star (Figure 4). At $g = 19.72 \pm 0.02$, HVS14, like HVS13, has a very large Galactocentric distance $R = 110$ kpc.

**Table 1**
HVS Survey Stars with $v_{rf} > +275$ KM S$^{-1}$

| ID | Type | $M_V$ (mag) | $V$ (mag) | $R_{GC}$ (kpc) | $l$ (deg) | $b$ (deg) | $v_\odot$ (km s$^{-1}$) | $v_{rf}$ (km s$^{-1}$) | Catalog |
|---|---|---|---|---|---|---|---|---|---|
| | | | | | HVSs | | | | |
| HVS1 | B | −0.3 | 19.83 | 111 | 227.33 | +31.33 | 840 | 696 | SDSS J090744.99+024506.9[1] |
| HVS2 | sdO | +2.6 | 19.05 | 26 | 175.99 | +47.05 | 708 | 717 | US 708[2] |
| HVS3 | B | −2.7 | 16.20 | 62 | 263.04 | −40.91 | 723 | 548 | HE 0437-5439[3] |
| HVS4 | B | −0.9 | 18.50 | 82 | 194.76 | +42.56 | 611 | 566 | SDSS J091301.01+305119.8[4] |
| HVS5 | B | −0.3 | 17.70 | 45 | 146.23 | +38.70 | 553 | 649 | SDSS J091759.48+672238.3[4] |
| HVS6 | B | −0.3 | 19.11 | 78 | 243.12 | +59.56 | 626 | 528 | SDSS J110557.45+093439.5[5] |
| HVS7 | B | −1.1 | 17.80 | 60 | 263.83 | +57.95 | 529 | 416 | SDSS J113312.12+010824.9[5] |
| HVS8 | B | −0.3 | 18.09 | 53 | 211.70 | +46.33 | 489 | 407 | SDSS J094214.04+200322.1[6] |
| HVS9 | B | −0.3 | 18.76 | 68 | 244.63 | +44.38 | 628 | 485 | SDSS J102137.08−005234.8[6] |
| HVS10 | B | −0.3 | 19.36 | 87 | 249.93 | +75.72 | 478 | 432 | SDSS J120337.85+180250.4[6] |
| HVS11 | A | +0.6 | 19.70 | 70 | 238.76 | +40.63 | 482 | 336 | SDSS J095906.48+000853.4 |
| HVS12 | A/BHB | +0.6 | 19.76 | 70 | 247.11 | +52.46 | 552 | 429 | SDSS J105009.60+031550.7 |
| HVS13 | B | −0.3 | 20.16 | 125 | 251.65 | +50.64 | 575 | 443 | SDSS J105248.31−000133.9 |
| HVS14 | B | −0.3 | 19.89 | 112 | 241.78 | +53.20 | 532 | 416 | SDSS J104401.75+061139.0 |
| HVS15 | B | −0.3 | 19.33 | 85 | 266.51 | +55.92 | 463 | 343 | SDSS J113341.09−012114.2 |
| HVS16 | B | −0.3 | 19.49 | 90 | 285.86 | +67.38 | 443 | 367 | SDSS J122523.40+052233.8 |
| | | | | | Possible HVSs | | | | |
| | A | +1.3 | 20.18 | 65 | 162.98 | +46.34 | 235 | 279 | SDSS J094014.56+530901.7 |
| | A | +0.6 | 19.95 | 79 | 155.49 | +49.45 | 228 | 289 | SDSS J101359.79+563111.7 |
| | A | +0.6 | 19.54 | 59 | 0.14 | +69.28 | 279 | 289 | SDSS J140306.54+145005.0 |
| | A | +0.6 | 20.30 | 83 | 39.36 | +50.87 | 193 | 293 | SDSS J154556.10+243708.9 |
| | | | | | Possible Bound HVSs | | | | |
| | B | −0.3 | 17.38 | 40 | 189.17 | −48.75 | 314 | 279 | SDSS J032054.69−060616.0 |
| | B | −0.3 | 18.56 | 66 | 196.07 | +23.21 | 361 | 298 | SDSS J074950.24+243841.2 |
| | B | −0.3 | 17.43 | 42 | 160.45 | +34.20 | 229 | 288 | SDSS J081828.07+570922.1 |
| | B | −0.3 | 18.23 | 57 | 186.30 | +42.16 | 306 | 285 | SDSS J090710.08+365957.5 |
| | B | −0.3 | 18.13 | 51 | 251.20 | +54.36 | 451 | 331 | SDSS J110224.37+025002.8 |
| | B | −0.3 | 18.31 | 53 | 274.88 | +57.45 | 424 | 310 | SDSS J115245.91−021116.2 |
| | B | −0.3 | 17.64 | 39 | 65.34 | +72.37 | 228 | 298 | SDSS J140432.38+352258.4 |
| | A | +0.0 | 18.56 | 49 | 357.16 | +63.62 | 284 | 290 | SDSS J141723.34+101245.7 |

**References.** (1) Brown et al. 2005; (2) Hirsch et al. 2005; (3) Edelmann et al. 2005; (4) Brown et al. 2006a; (5) Brown et al. 2006b; (6) Brown et al. 2007b.

SDSS J113341.09−012114.25, hereafter HVS15, has a B9 spectral type, a 463 ± 11 km s$^{-1}$ heliocentric radial velocity, and a minimum velocity of 343 km s$^{-1}$ in the Galactic rest frame. HVS15 is the bluest of the new HVSs with $(g' - r')_0 = -0.346 \pm 0.031$, consistent with a 3 $M_\odot$ main-sequence star. We previously classified HVS15 as a possibly bound HVS (Brown et al. 2007b), but in light of its probable $R = 85$ kpc distance the star is almost certainly unbound. HVS15 would be located at $R = 37$ kpc if it were a hot BHB star, yet its minimum rest-frame velocity would still be in excess of the Xue et al. (2008) Galactic escape velocity estimate (see Figure 3).

SDSS J122523.40+052233.85, hereafter HVS16, has a B9 spectral type, a 443 ± 14 km s$^{-1}$ heliocentric radial velocity, and a minimum velocity of 367 km s$^{-1}$ in the Galactic rest frame. Its broadband colors are consistent with a 3 $M_\odot$ main-sequence star, which places HVS16 at an approximate Galactocentric distance $R = 90$ kpc. Similar to HVS15, HVS16 would be located about $R = 44$ kpc if it were a hot BHB star, but its minimum rest-frame velocity would still be in excess of the Xue et al. (2008) Galactic escape velocity estimate. We conclude that both HVS15 and HVS16 are very likely unbound.

### 4.2. Four Possible HVSs

There are four HVS candidates with minimum rest-frame velocities, main-sequence star distances, and BHB star distances that fall between the Kenyon et al. (2008) and Xue et al. (2008) Galactic escape velocity models. In other words, these stars are unambiguously bound in the Kenyon et al. (2008) model, and unambiguously unbound in the Xue et al. (2008) model.

The four possible HVSs are SDSS J094014.56+530901.74, SDSS J101359.79+563111.66, SDSS J141342.50+442550.03, and SDSS J154556.10+243708.94. All four stars have minimum rest-frame velocities around +290 km s$^{-1}$ and the spectral types of early A-type stars. These four possible HVSs are systematically redder than the other HVSs, consistent with 2–2.5 $M_\odot$ stars (see Figure 1). Their main-sequence star and BHB distances range 55–85 kpc (see Figure 3).

Although the four stars are very possibly unbound, an HVS origin is not a unique explanation for their velocities. As explained above, runaway ejections can "contaminate" the low-velocity end of HVSs. It is, however, more likely that unbound low-mass A stars are ejected by an MBH. Proper motions are needed to distinguish these four stars as HVSs or runaways.

### 4.3. HVS Table

Table 1 lists the 26 stars in our HVS survey with $v_{rf} > +275$ km s$^{-1}$, plus HVS2 and HVS3 for completeness. Magnitudes and radial velocities are observed quantities, whereas luminosities and distances are inferred from spectra and colors. Columns include HVS number, stellar type, absolute

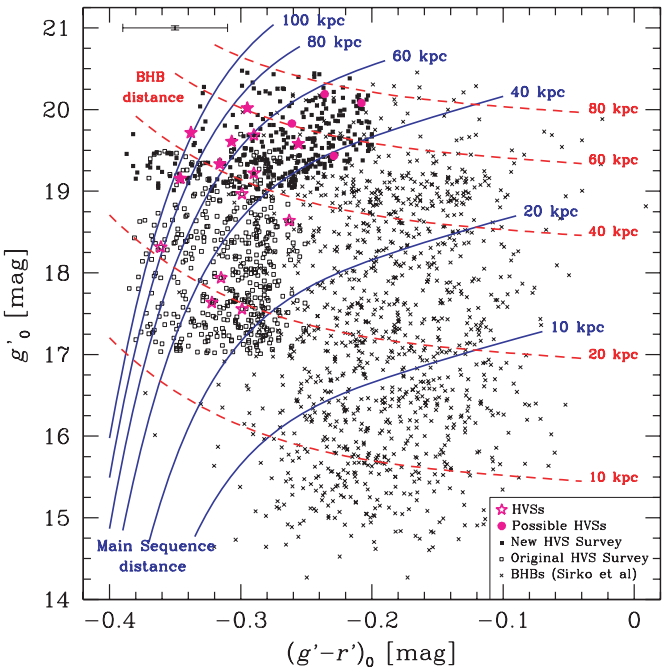


**Figure 5.** Color–magnitude diagram showing that the original HVS survey stars (open squares) are by design bluer than Sirko et al. (2004a) BHB stars (crosses), while the new HVS survey stars (solid squares) are systematically fainter than the BHB stars. We plot SDSS DR6 uber-calibrated PSF magnitudes, corrected for Galactic extinction, for all stars. Lines indicate the distance for main-sequence stars with solar abundance (solid lines, Girardi et al. 2002, 2004) and for halo BHB stars with [Fe/H]= −1.7 (dashed lines, Brown et al. 2008).

(A color version of this figure is available in the online journal.)

magnitude $M_V$, apparent $V$ magnitude derived from SDSS photometry, Galactocentric distance $R$, Galactic coordinates $(l, b)$, heliocentric radial velocity $v_\odot$, minimum Galactic rest-frame velocity $v_{rf}$ (not a full space velocity), and catalog identification. We report the weighted average velocity measurements for each object. Thus the velocities in Table 1 may vary slightly from earlier work.

We do not report errors in Table 1 because formal uncertainties are misleadingly small compared to the (unknown) systematic errors. For example, our radial velocities have 11–17 km s$^{-1}$ uncertainties, but we have no constraint on the proper motion component of the rest-frame velocity $v_{rf}$. The luminosity estimates are precise at the 10% level for main-sequence stars. However, the luminosity estimates could be overestimated by an order of magnitude for post–main-sequence stars.

## 5. THE NATURE OF HYPERVELOCITY STARS

We argued previously that HVSs must be short-lived main-sequence stars (Brown et al. 2007b). Follow-up observations have, remarkably, confirmed that four B-type HVSs are main-sequence stars: HVS1 is a slowly pulsating B variable (Fuentes et al. 2006), HVS3 is a 9 $M_\odot$ B star (Bonanos et al. 2008; Przybilla et al. 2008b), HVS7 is a 3.7 $M_\odot$ Bp star (Przybilla et al. 2008c), and HVS8 is a rapidly rotating B star (Lopez-Morales & Bonanos 2008).

The identification of HVSs as main-sequence stars is in stark contrast to the halo stars in our survey, which are presumably evolved 0.6–1 $M_\odot$ stars on the BHB. BHB stars among the HVSs would be exciting, however, because unbound BHB stars would allow us to probe the low-mass regime of HVSs.

Kenyon et al. (2008) calculate the observable spatial and velocity distribution of HVSs as a function of mass, and predict that BHB stars are ∼ 10 times less abundant than main-sequence HVSs. Roughly speaking, solar mass HVSs are 10 times more abundant than 3–4 $M_\odot$ HVSs, but spend 1% of their lifetime in the BHB phase with luminosity comparable to an 2.5 $M_\odot$ main-sequence star. Not all of our HVSs have the colors of a 2.5 $M_\odot$ main-sequence star (see Figure 1). Yet, given the 16–20 HVSs identified to date, the predictions of Kenyon et al. (2008) imply that there should be 1±1 BHB stars among our HVSs.

### 5.1. A Possible BHB HVS

BHB stars and main-sequence stars are distinguished by surface gravity: low surface gravity BHB stars have narrower Balmer lines (at a given effective temperature) than high surface gravity main-sequence stars. Spectroscopic measures of surface gravity work for temperatures cooler (redder) than $(B-V)_0 = 0$ (e.g., Kinman et al. 1994; Wilhelm et al. 1999; Clewley et al. 2002), colors that we probe now with our new HVS survey.

Applying the Clewley et al. (2002, 2004) surface gravity measures to the new HVSs, HVS12 is a possible BHB star. The line width-shape technique indicates HVS12 has low surface gravity, although the $D_{0.15}$-color technique is ambiguous because of HVS12's blue $(B-V)_0 = -0.05 \pm 0.04$ color. If HVS12 is a BHB star with [Fe/H]= −1.5, then it has $M_V$(BHB) ≃ +1.2 (Brown et al. 2008) and is located at $R \simeq 50$ kpc. HVS12 is clearly unbound at this distance (see Figure 3).

Interestingly, HVS12 was previously classified as a BHB star by Sirko et al. (2004a). Sirko et al. published a sample of 1170 BHB stars observed as misidentified quasars and filler objects in the SDSS spectroscopic survey. For HVS12 they report a 532 ± 35 km s$^{-1}$ heliocentric velocity and a 0.847 Ca II K equivalent width, consistent at the 1$\sigma$ level with our own measurements. Xue et al. (2008) have recently reanalyzed the SDSS BHB sample and combined it with additional targeted observations from the SEGUE survey. Xue et al. (2008) classify HVS12 as a possible BHB star, but exclude it from the their rigorously selected BHB sample. High S/N spectroscopy and photometry is required to confirm the nature of HVS12.

Although HVS12 is a clear outlier in the velocity distribution of BHB stars (see Figure 4 of Sirko et al. 2004b), HVS12 was not previously recognized as an unbound star. The median depth of the Sirko et al. (2004a) sample is $g'_0 = 17.35$, corresponding to a distance of ∼20 kpc for a BHB star (see Figure 5). A star with $v_{rf} \sim 400$ km s$^{-1}$ at the median depth of the Sirko et al. (2004a) sample is thus bound. What appears to have escaped notice, however, is that HVS12 is fainter, and bluer, than 96% of the Sirko et al. (2004a) BHB sample.

Figure 5 compares the distribution of stars in our HVS surveys and the Sirko et al. (2004a) BHB sample in a color–magnitude diagram. For reference, we draw lines of constant distance for main-sequence stars with solar abundance (solid lines; Girardi et al. 2002, 2004) and for halo BHB stars with [Fe/H]= −1.7 (dashed lines; Brown et al. 2008). Note that the color–magnitude selection of the new HVS survey is such that every star has $R \gtrsim 40$ kpc, whether a main-sequence star or a BHB star (Figure 5).

The presence of only one HVS among the 1170 Sirko et al. (2004a) BHB stars and the 10224 Xue et al. (2008) BHB candidates shows the immense dilution due to stars in the Galactic halo. It is important to minimize contamination from foreground stellar populations when looking for HVSs. Our surveys find HVSs because we target stars that are bluer and/or fainter than the bulk of halo BHB stars.

## 6. CONCLUSIONS

We describe a new targeted HVS survey, a spectroscopic survey of faint stars $19 < g_0' < 20.5$ with early A-type and late B-type colors. Recent observations confirm that three of our B-type HVSs are 3–4 $M_\odot$ main-sequence stars.

The observational signature of an HVS is its unbound velocity, which we determine by comparing observed radial velocities and distances to Galactic potential models. We argue that the known properties of binaries and the rarity of massive stars make hyper-runaways like HD 271791 rare. An MBH ejection remains the most plausible origin of unbound low-mass stars.

Our HVS survey is 59% complete and, combined with our original HVS survey, shows a remarkable velocity distribution: 26 stars with $v_{rf} > +275$ km s$^{-1}$ and only two stars with $v_{rf} < -275$ km s$^{-1}$. Here we report the discovery of six new unbound HVSs in excess of the conservative escape velocity model of Kenyon et al. (2008), and four additional unbound HVSs in excess of the escape velocity model of Xue et al. (2008).

One of the new HVSs may be an evolved BHB star. The Kenyon et al. (2008) ejection models predict BHB HVSs are ∼10 times less abundant than the main-sequence HVSs in our survey, consistent with the existence of $1 \pm 1$ BHB stars in our HVS sample. Of course, the exact number of BHB HVSs depends on the mass function of stars near the central MBH. BHB HVSs therefore have the potential to probe the low-mass regime of HVSs and constrain the mass function of stars in the Galactic center.

HVSs are fascinating because their properties are tied to the nature and environment of the MBH that ejects them (Levin 2006; Baumgardt et al. 2006; Merritt 2006; Ginsburg & Loeb 2006, 2007; Demarque & Virani 2007; Gualandris & Portegies Zwart 2007; Sesana et al. 2006, 2007a, 2007b, 2008; Lu et al. 2007; Kollmeier & Gould 2007; Hansen 2007; Perets et al. 2008; Perets 2008, 2009; Perets & Alexander 2008; Sherwin et al. 2008; Svensson et al. 2008; O'Leary & Loeb 2008; Löckmann & Baumgardt 2008), and their trajectories probe the dark matter halo through which they move (Gnedin et al. 2005; Yu & Madau 2007; Wu et al. 2008; Kenyon et al. 2008). The angular distribution of HVSs on the sky reveals significant anisotropy that may also be related to the Galactic potential (Brown et al. 2009). Our ultimate goal is to find a statistical sample of ∼100 HVSs to measure the distribution of HVS properties and discriminate HVS ejection models.

We thank M. Alegria and A. Milone for their assistance with observations obtained at the MMT Observatory, a joint facility of the Smithsonian Institution and the University of Arizona. This project makes use of data products from the SDSS, which is managed by the Astrophysical Research Consortium for the Participating Institutions. This research makes use of NASA's Astrophysics Data System Bibliographic Services. This work was supported by the Smithsonian Institution.

*Facilities:* MMT (Blue Channel Spectrograph)

## APPENDIX.

## DATA TABLE

Table 2 presents the 19 $z \sim 2.4$ quasars and the nine DA white dwarfs in our survey. Table columns include right ascension and decl. coordinates (J2000), $g'$ apparent magnitude, $(u'-g')_0$ and $(g'-r')_0$ color, and spectroscopic identification.

**Table 2**
Quasars and White Dwarfs

| R.A. (hr) | Decl. (deg) | $g'$ (mag) | $(u'-g')_0$ (mag) | $(g'-r')_0$ (mag) | Type |
|---|---|---|---|---|---|
| 4:06:24.10 | −4 : 19 : 34.0 | 20.594 | 0.763 | −0.268 | QSO |
| 8:05:30.10 | 2 : 18 : 45.0 | 20.448 | 0.804 | −0.225 | QSO |
| 8:06:21.42 | 33 : 38 : 32.8 | 19.993 | 0.649 | −0.244 | WD |
| 8:23:36.89 | 1 : 52 : 55.9 | 20.445 | 0.873 | −0.220 | QSO |
| 9:03:21.90 | 49 : 51 : 49.0 | 20.315 | 0.639 | −0.276 | WD |
| 9:19:14.83 | 12 : 52 : 06.0 | 20.014 | 0.725 | −0.250 | WD |
| 9:22:11.31 | 45 : 57 : 19.4 | 20.244 | 0.900 | −0.270 | QSO |
| 9:52:18.52 | 33 : 24 : 46.4 | 20.110 | 0.638 | −0.250 | WD |
| 10:00:52.77 | 40 : 51 : 23.3 | 20.078 | 1.021 | −0.216 | QSO |
| 10:18:11.91 | 50 : 16 : 00.9 | 20.422 | 0.611 | −0.292 | QSO |
| 10:42:58.03 | 28 : 30 : 33.4 | 20.361 | 1.000 | −0.344 | QSO |
| 10:45:01.96 | −1 : 19 : 46.7 | 20.284 | 0.673 | −0.263 | QSO |
| 11:02:16.15 | 7 : 54 : 20.7 | 19.773 | 0.853 | −0.211 | QSO |
| 11:10:19.82 | 59 : 14 : 59.3 | 19.753 | 0.887 | −0.291 | QSO |
| 11:18:54.44 | 30 : 27 : 09.9 | 20.366 | 0.757 | −0.239 | QSO |
| 11:41:02.74 | 42 : 20 : 34.0 | 20.561 | 0.847 | −0.337 | QSO |
| 11:56:56.37 | 22 : 41 : 55.3 | 20.141 | 0.794 | −0.271 | QSO |
| 11:57:26.83 | −1 : 29 : 14.9 | 19.872 | 0.610 | −0.271 | WD |
| 12:15:53.64 | 34 : 23 : 18.2 | 20.058 | 0.831 | −0.223 | QSO |
| 12:29:08.32 | 49 : 58 : 27.2 | 20.416 | 0.961 | −0.213 | QSO |
| 13:07:54.94 | 48 : 35 : 25.9 | 20.168 | 0.661 | −0.238 | QSO |
| 14:13:42.51 | 44 : 25 : 50.0 | 20.457 | 0.807 | −0.224 | QSO |
| 14:22:00.74 | 43 : 52 : 53.2 | 19.821 | 0.715 | −0.271 | WD |
| 15:33:00.04 | 49 : 29 : 48.3 | 19.278 | 0.611 | −0.248 | WD |
| 15:43:24.56 | 36 : 26 : 49.5 | 19.599 | 0.926 | −0.275 | QSO |
| 15:58:51.85 | 22 : 21 : 59.9 | 19.671 | 0.817 | −0.292 | QSO |
| 16:11:27.35 | 26 : 56 : 10.9 | 19.977 | 0.647 | −0.305 | WD |
| 17:40:43.32 | 67 : 24 : 41.5 | 19.680 | 0.663 | −0.268 | WD |

## REFERENCES

Abt, H. A., Levato, H., & Grosso, M. 2002, ApJ, 573, 359
Arzoumanian, Z., Chernoff, D. F., & Cordes, J. M. 2002, ApJ, 568, 289
Baumgardt, H., Gualandris, A., & Portegies Zwart, S. 2006, MNRAS, 372, 174
Behr, B. B. 2003a, ApJS, 149, 67
Behr, B. B. 2003b, ApJS, 149, 101
Blaauw, A. 1961, Bull. Astron. Inst. Netherlands, 15, 265
Bonanos, A. Z., López-Morales, M., Hunter, I., & Ryans, R. S. I. 2008, ApJ, 675, L77
Bromley, B. C., Kenyon, S. J., Geller, M. J., Barcikowski, E., Brown, W. R., & Kurtz, M. J. 2006, ApJ, 653, 1194
Brown, W. R., Beers, T. C., Wilhelm, R., Allende Prieto, C., Geller, M. J., Kenyon, S. J., & Kurtz, M. J. 2008, AJ, 135, 564
Brown, W. R., Geller, M. J., Kenyon, S. J., & Bromley, B. C. 2009, ApJ, 690, L69
Brown, W. R., Geller, M. J., Kenyon, S. J., & Kurtz, M. J. 2005, ApJ, 622, L33
Brown, W. R., Geller, M. J., Kenyon, S. J., & Kurtz, M. J. 2006a, ApJ, 640, L35
Brown, W. R., Geller, M. J., Kenyon, S. J., & Kurtz, M. J. 2006b, ApJ, 647, 303
Brown, W. R., Geller, M. J., Kenyon, S. J., Kurtz, M. J., & Bromley, B. C. 2007a, ApJ, 660, 311
Brown, W. R., Geller, M. J., Kenyon, S. J., Kurtz, M. J., & Bromley, B. C. 2007b, ApJ, 671, 1708
Carollo, D., et al. 2007, Nature, 450, 1020
Clewley, L., Warren, S. J., Hewett, P. C., Norris, J. E., & Evans, N. W. 2004, MNRAS, 352, 285
Clewley, L., Warren, S. J., Hewett, P. C., Norris, J. E., Peterson, R. C., & Evans, N. W. 2002, MNRAS, 337, 87
Clewley, L., Warren, S. J., Hewett, P. C., Norris, J. E., Wilkinson, M. I., & Evans, N. W. 2005, MNRAS, 362, 349
Davies, M. B., King, A., & Ritter, H. 2002, MNRAS, 333, 463
Demarque, P., & Virani, S. 2007, A&A, 461, 651
Dolphin, A. E., et al. 2003, AJ, 125, 1261
Edelmann, H., Napiwotzki, R., Heber, U., Christlieb, N., & Reimers, D. 2005, ApJ, 634, L181
Fossati, L., et al. 2007, A&A, 476, 911
Fregeau, J. M., Cheung, P., Portegies Zwart, S. F., & Rasio, F. A. 2004, MNRAS, 352, 1

Fuentes, C. I., Stanek, K. Z., Gaudi, B. S., McLeod, B. A., Bogdanov, S., Hartman, J. D., Hickox, R. C., & Holman, M. J. 2006, ApJ, 636, L37
Gebran, M., & Monier, R. 2008, A&A, 483, 567
Gebran, M., Monier, R., & Richard, O. 2008, A&A, 479, 189
Ghez, A. M., et al. 2008, ApJ, 689, 1044
Ginsburg, I., & Loeb, A. 2006, MNRAS, 368, 221
Ginsburg, I., & Loeb, A. 2007, MNRAS, 376, 492
Girardi, L., Bertelli, G., Bressan, A., Chiosi, C., Groenewegen, M. A. T., Marigo, P., Salasnich, B., & Weiss, A. 2002, A&A, 391, 195
Girardi, L., Grebel, E. K., Odenkirchen, M., & Chiosi, C. 2004, A&A, 422, 205
Gnedin, O. Y., Gould, A., Miralda Escudé, J., & Zentner, A. R. 2005, ApJ, 634, 344
Gualandris, A., & Portegies Zwart, S. 2007, MNRAS, 376, L29
Gualandris, A., Portegies Zwart, S., & Sipior, M. S. 2005, MNRAS, 363, 223
Gvaramadze, V. V., Gualandris, A., & Portegies Zwart, S. 2008, MNRAS, 385, 929
Hansen, B. M. S. 2007, ApJ, 671, L133
Heber, U., Edelmann, H., Napiwotzki, R., Altmann, M., & Scholz, R.-D. 2008a, A&A, 483, L21
Heber, U., Hirsch, H., Edelmann, H., Napiwotzki, R., O'Toole, S., Brown, W., & Altmann, M. 2008b, in APS Conf. Ser. 392, Hot Subdwarf Stars and Related Objects, ed. U. Heber, C. S. Jeffery, & R. Napiwotski (San Francisco, CA: ASP), 167
Hills, J. G. 1988, Nature, 331, 687
Hirsch, H. A., Heber, U., O'Toole, S. J., & Bresolin, F. 2005, A&A, 444, L61
Huang, W., & Gies, D. R. 2006, ApJ, 648, 580
Jurić, M., et al. 2008, ApJ, 673, 864
Kenyon, S. J., Bromley, B. C., Geller, M. J., & Brown, W. R. 2008, ApJ, 680, 312
Kinman, T. D., Suntzeff, N. B., & Kraft, R. P. 1994, AJ, 108, 1722
Kobulnicky, H. A., & Fryer, C. L. 2007, ApJ, 670, 747
Kollmeier, J. A., & Gould, A. 2007, ApJ, 664, 343
Kurtz, M. J., & Mink, D. J. 1998, PASP, 110, 934
Lada, C. J., & Lada, E. A. 2003, ARA&A, 41, 57
Lee, H. M., & Ostriker, J. P. 1986, ApJ, 310, 176
Leonard, P. J. T. 1991, AJ, 101, 562
Leonard, P. J. T. 1993, in ASP Conf. Ser. 45, Luminous High-Latitude Stars, ed. D. Sasselov (San Francisco, CA: ASP), 360
Leonard, P. J. T., & Duncan, M. J. 1988, AJ, 96, 222
Levin, Y. 2006, ApJ, 653, 1203
Löckmann, U., & Baumgardt, H. 2008, MNRAS, 384, 323
Lopez-Morales, M., & Bonanos, A. Z. 2008, ApJ, accepted
Lu, Y., Yu, Q., & Lin, D. N. C. 2007, ApJ, 666, L89
McMillan, S. L. W., McDermott, P. N., & Taam, R. E. 1987, ApJ, 318, 261
Merritt, D. 2006, ApJ, 648, 976
Monier, R. 2005, A&A, 442, 563
Morrison, H. L., et al. 2008, ApJ, submitted, arXiv:0804.2448
O'Leary, R. M., & Loeb, A. 2008, MNRAS, 383, 86
Perets, H. B. 2008, arXiv:0802.1004
Perets, H. B. 2009, ApJ, 690, 795
Perets, H. B., & Alexander, T. 2008, ApJ, 677, 146
Perets, H. B., Hopman, C., & Alexander, T. 2007, ApJ, 656, 709
Portegies Zwart, S. F. 2000, ApJ, 544, 437
Poveda, A., Ruiz, J., & Allen, C. 1967, Bol. Obs. Tonantzintla Tacubaya, 4, 860
Przybilla, N., Nieva, M. F., Heber, U., & Butler, K. 2008a, ApJ, accepted
Przybilla, N., Nieva, M. F., Heber, U., Firnstein, M., Butler, K., Napiwotzki, R., & Edelmann, H. 2008b, A&A, 480, L37
Przybilla, N., Nieva, M. F., Tillich, A., Heber, U., Butler, K., & Brown, W. R. 2008c, A&A, accepted
Salpeter, E. E. 1955, ApJ, 121, 161
Schaller, G., Schaerer, D., Meynet, G., & Maeder, A. 1992, A&AS, 96, 269
Schödel, R., Ott, T., Genzel, R., Eckart, A., Mouawad, N., & Alexander, T. 2003, ApJ, 596, 1015
Sesana, A., Haardt, F., & Madau, P. 2006, ApJ, 651, 392
Sesana, A., Haardt, F., & Madau, P. 2007a, ApJ, 660, 546
Sesana, A., Haardt, F., & Madau, P. 2007b, MNRAS, 379, L45
Sesana, A., Haardt, F., & Madau, P. 2008, ApJ, 686, 432
Sherwin, B. D., Loeb, A., & O'Leary, R. M. 2008, MNRAS, 386, 1179
Siegel, M. H., Majewski, S. R., Reid, I. N., & Thompson, I. B. 2002, ApJ, 578, 151
Sirko, E., et al. 2004a, AJ, 127, 899
Sirko, E., et al. 2004b, AJ, 127, 914
Svensson, K. M., Church, R. P., & Davies, M. B. 2008, MNRAS, 383, L15
Tauris, T. M., & Takens, R. J. 1998, A&A, 330, 1047
Vanbeveren, D., De Loore, C., & Van Rensbergen, W. 1998, A&A Rev., 9, 63
Varenne, O., & Monier, R. 1999, A&A, 351, 247
Wilhelm, R., Beers, T. C., & Gray, R. O. 1999, AJ, 117, 2308
Wu, X., Famaey, B., Gentile, G., Perets, H., & Zhao, H. 2008, MNRAS, 386, 2199
Xue, X., et al. 2008, ApJ, 684, 1143
Young, L. M. 2000, AJ, 119, 188
Yu, Q., & Madau, P. 2007, MNRAS, 379, 1293
Yu, Q., & Tremaine, S. 2003, ApJ, 599, 1129